The Journal of Chemical Physics

Infrared spectroscopy of RG–$Co^+(H_2O)$ complexes (RG = Ar, Ne, He): The role of rare gas "tag" atoms

Cite as: J. Chem. Phys. **154**, 064306 (2021); https://doi.org/10.1063/5.0041069
Submitted: 18 December 2020 • Accepted: 17 January 2021 • Published Online: 11 February 2021

Joshua H. Marks, Evangelos Miliordos and Michael A. Duncan

View Online Export Citation CrossMark

ARTICLES YOU MAY BE INTERESTED IN

Invited Review Article: Laser vaporization cluster sources
Review of Scientific Instruments **83**, 041101 (2012); https://doi.org/10.1063/1.3697599

IR multiple photon dissociation spectroscopy of MO_2^+ (M = V, Nb, Ta)
The Journal of Chemical Physics **153**, 171101 (2020); https://doi.org/10.1063/5.0024675

Argon tagging of doubly transition metal doped aluminum clusters: The importance of electronic shielding
The Journal of Chemical Physics **154**, 054312 (2021); https://doi.org/10.1063/5.0037568

Lock-in Amplifiers up to 600 MHz
Zurich Instruments
Watch

AIP Publishing

© 2021 Author(s).

The Journal of Chemical Physics ARTICLE scitation.org/journal/jcp

Infrared spectroscopy of RG–$Co^+(H_2O)$ complexes (RG = Ar, Ne, He): The role of rare gas "tag" atoms

Cite as: J. Chem. Phys. 154, 064306 (2021); doi: 10.1063/5.0041069
Submitted: 18 December 2020 • Accepted: 17 January 2021 •
Published Online: 11 February 2021

View Online Export Citation CrossMark

Joshua H. Marks,[1] Evangelos Miliordos,[2] and Michael A. Duncan[1,a)]

AFFILIATIONS

[1] Department of Chemistry, University of Georgia, Athens, Georgia 30602, USA
[2] Department of Chemistry and Biochemistry, Auburn University, Auburn, Alabama 36849, USA

[a)] Author to whom correspondence should be addressed: maduncan@uga.edu

ABSTRACT

RG_n–$Co^+(H_2O)$ cation complexes (RG = Ar, Ne, He) are generated in a supersonic expansion by pulsed laser vaporization. Complexes are mass-selected using a time-of-flight spectrometer and studied with infrared laser photodissociation spectroscopy, measuring the respective mass channels corresponding to the elimination of the rare gas "tag" atom. Spectral patterns and theory indicate that the structures of the ions with a single rare gas atom have this bound to the cobalt cation opposite the water moiety in a near-C_{2v} arrangement. The O–H stretch vibrations of the complex are shifted compared to those of water because of the metal cation charge-transfer interaction; these frequencies also vary systematically with the rare gas atom attached. The efficiencies of photodissociation also vary with the rare gas atoms because of their widely different binding energies to the cobalt cation. The spectrum of the argon complex could only be measured when at least three argon atoms were attached. In the case of the helium complex, the low binding energy allows the spectra to be measured for the low-frequency H–O–H scissors bending mode and for the O–D stretches of the deuterated analog. The partially resolved rotational structure for the antisymmetric O–H and O–D stretches reveals the temperature of these complexes (6 K) and establishes the electronic ground state. The helium complex has the same $^3B_1$ ground state as the tag-free complex studied previously by Metz and co-workers ["Dissociation energy and electronic and vibrational spectroscopy of $Co^+(H_2O)$ and its isotopomers," J. Phys. Chem. A **117**, 1254 (2013)], but the *A* rotational constant is contaminated by vibrational averaging from the bending motion of the helium.

Published under license by AIP Publishing. https://doi.org/10.1063/5.0041069

INTRODUCTION

Metal cation solvation by water occurs in numerous contexts throughout chemistry and biology.[1,2] The binding of the individual water molecules interacting with a metal ion determines their structures, how they bind to and polarize subsequent molecules in the coordination/solvation sphere, and the mobility of ions moving through solution. Unfortunately, these molecular details of coordination and solvation are extremely difficult to measure in solution. Consequently, isolated metal ion–water complexes of finite size have been studied and modeled with theory to elucidate this chemistry. The reactions and energetics of metal ion–water complexes have been studied in the gas phase using mass spectrometry.[3–20] Computational studies have provided insight into structures of complexes in various charge states and with different numbers of water molecules interacting with the metal.[21–37] Spectroscopic studies have combined mass spectrometry and laser excitation in either the UV–visible[38–50] or infrared regions[50–78] using the method of photodissociation spectroscopy. Many photodissociation experiments employ rare gas atom "tagging" to enhance photodissociation yields with the hope that this will not adversely perturb the intrinsic structure and spectroscopy of the system. Ions with strong bonding may not photodissociate efficiently, but if a weakly bound rare gas atom is attached, it can be eliminated upon optical excitation, providing an efficient way to detect absorption. However, the effects of tagging are not often investigated or documented. In this report, we

Published under license by AIP Publishing

employ infrared photodissociation spectroscopy and computational studies on the cobalt–water cation complex tagged with different rare gas atoms to investigate the effects of tagging on the structure and spectroscopy of this system.

Metal ion–water complexes have been studied extensively, and many of their structural and spectroscopic properties are well documented. In mass spectrometry, methods such as collision-induced dissociation (CID) have been employed to determine binding energies.[4–6,9,14,15,18–20] Computational studies elucidate binding energetics and structures, including the role of specific metal ion spin states in bonding.[21–37] Infrared spectroscopic studies have revealed that significant charge transfer occurs from the water toward the metal cation in these complexes.[50–78] Related to this charge transfer, the bonding electron density of water is redistributed, producing corresponding changes to vibrational frequencies and intensities. The O–H stretches generally shift to frequencies 30–50 cm^{-1}, lower than those of the isolated water molecule, and the usually weak symmetric stretch becomes comparable in intensity to the antisymmetric stretch. Additionally, the partially resolved rotational structure seen for certain complexes shows that the water molecules are distorted structurally by the binding to metal, with expansion of the H–O–H bond angle.[52,58,60,66,75–77] In multi-water complexes, the coordination numbers have been determined.[57,59,61–63,65,68–71,73,77,78] The gas phase values for coordination numbers around singly charged cations (3-4 molecules) are generally lower than those expected for corresponding di-cations in solution.

The $Co^+(H_2O)$ complex is a particularly interesting system with which we study rare gas atom tagging interactions. The spectroscopy of this ion has been studied previously by Metz and co-workers,[50] who obtained rotationally resolved electronic spectroscopy for the tag-free complex. IR-optical double resonance experiments measured the O–H stretch vibrations.[50] Ohashi and co-workers studied larger $Co^+(H_2O)_n$ complexes (n = 4–6) via infrared photodissociation and the elimination of water molecules.[69] Because of *d* electron contraction, the cobalt cation and other late-period transition metal cations have small ionic radii, resulting in strong ion-induced dipole bonds to rare gas atoms.[79–82] Electronic spectroscopy of Co^+–Ar by Brucat and co-workers found a dissociation energy of 4200 cm^{-1},[79] whereas a similar measurement of Co^+–Ne by our group found a dissociation energy of 930 cm^{-1}.[82] Computational studies have suggested that the bond energy of Co^+–He would be only somewhat smaller than that of Co^+–Ne.[80,81] These energetics suggest that complexes of each of these rare gases could be formed with $Co^+(H_2O)$, allowing a study of its spectroscopy and the dependence on the tag atom employed. In the present work, we describe such a study by infrared photodissociation of various RG–$Co^+(H_2O)$ complexes.

EXPERIMENTAL AND COMPUTATIONAL DETAILS

RG–$Co^+(H_2O)$ complexes are produced in a pulsed supersonic expansion by laser vaporization.[83] Pure rare gas expansions were used for the argon and helium complexes; a 70:30 mix of Ne:He was employed for the neon complexes. The rare gas was passed through tubing containing a few drops of water at room temperature before expansion into vacuum. Laser vaporization was accomplished with a Spectra Physics INDI laser operated at 355 nm, using the so-called "off-set" sample rod configuration,[83] with a rotating metal rod mounted at a position displaced a few mm from the main expansion-gas flow axis. Mass analysis and selection were carried out using a reflectron time-of-flight spectrometer.[84] Mass-selected ions were studied by infrared photodissociation using a LaserVision OPO/OPA passing through the reflectron, and retro-reflected by a gold concave mirror producing a focal point on the ion beam. Spectra were measured by recording the elimination of He, Ne, or Ar from the respective RG–$Co^+(H_2O)$ complexes. Other details of the experiment are similar to those reported in our previous work.[77]

Computational studies were initially carried out at the complete active space self-consistent field (CASSCF) level with the MOLPRO computational package to generate potential energy curves and evaluate the multi-reference character of $Co^+(H_2O)$.[85] The active space consists of the eight valence electrons of Co^+ in 11 orbitals, which correspond to the 4*s*, 3*d*, and an additional set of *d* orbitals of cobalt at infinite separation. The latter orbitals were found to be necessary for smooth convergence. These calculations revealed single reference character in the equilibrium region of these complexes, and allowed us to obtain structures and energetics at the coupled cluster singles, doubles, and perturbatively connected triples [CCSD(T)] level of theory. The tagged He–$Co^+(H_2O)$, Ne–$Co^+(H_2O)$, and Ar_3–$Co^+(H_2O)$ species have relatively high (C_{2v} except for Ar_3) symmetry and were studied using the same methodology. The cc-pVTZ basis set is used for all of the atoms. The isotropic Fermi contact couplings and harmonic vibrational frequencies were obtained at the CCSD level in Gaussian 16.[86] Density Functional Theory (DFT) calculations were also done for the structural investigation of the larger Ar_3–$Co^+(H_2O)$ complex and the estimation of vibrationally averaged rotational constants of all species. For the latter, the VPT2 code was used as implemented in Gaussian 16. We selected the MN15 functional, since it has shown good performance for transition metal compounds and helped us bypass convergence issues with other functionals.[87] Scaling factors for the bend and stretches of water were determined with MN15 by comparing the frequencies computed for the isolated water molecule to its known experimental values.[88] A scaling factor of 1.001 was applied for the HOH bend, and a factor of 0.951 was applied for both O–H stretching modes. The MN15 functional has not been employed extensively to the vibrational frequencies of cation–molecular complexes. Therefore, we validated this method by applying it to the previously studied $Ti^+(H_2O)$ complex,[75] as described in the supplementary material (Table S4).

RESULTS AND DISCUSSION

Laser vaporization under conditions similar to those employed in previous work produced cation masses of the form RG_n-$Co^+(H_2O)_m$. The efficiency for attaching rare gas atoms to these complexes varied significantly with the three rare gases. As expected, argon binding was most efficient, allowing multiple atoms to be attached, whereas neon and helium complexes were more difficult to produce. Representative mass spectra for each of these systems are shown in the supplementary material (Figs. S1–S4). The use of

Published under license by AIP Publishing

the off-set configuration of the cluster source, in which the rotating sample rod is mounted slightly off to the side from the gas flow from the nozzle,[83] is critical to our ability to produce the neon and helium complexes. This configuration produces cold ions, but it also seems to limit the mobility of electrons from the vaporization plasma into the cold core of the supersonic expansion. This inhibits the rate of electron–ion recombination, which tends to neutralize the coldest ions.[83] With lower electron density here, a greater fraction of the coldest cations survive for the experiment.

Comparison of spectra in the O–H stretching region

Infrared photodissociation could not be detected for the Ar–$Co^+(H_2O)$ or Ar_2–$Co^+(H_2O)$ complexes in the O–H stretching region, presumably because the argon binding energy to cobalt in these complexes is too high. However, efficient photodissociation was detected for Ar_3–$Co^+(H_2O)$, producing the fragment ion corresponding to the loss of one argon atom. Likewise, the photodissociation of Ne–$Co^+(H_2O)$ was also extremely difficult to detect, even though the parent ion intensity was substantial. It is not clear whether the lack of dissociation here is caused by a high binding energy for neon or other factors. Fragmentation of the He–$Co^+(H_2O)$ complex via the loss of helium was relatively efficient.

The infrared photodissociation spectra of Ar_3–$Co^+(H_2O)$, Ne–$Co^+(H_2O)$, and He–$Co^+(H_2O)$ in the O–H stretching region are shown in Fig. 1. The argon complex spectrum has a greater signal level because of the larger abundance of the parent ion and the greater fragmentation yield than that found for the neon or helium complexes. Two bands in the argon complex spectrum are found at 3633 and 3707 cm^{-1}. The neon complex spectrum is very weak because of the extreme difficulty in fragmenting this ion. It has barely discernable features at 3615 and 3687 cm^{-1}. The helium complex spectrum has signal levels more like those of the argon complex, with a single band at 3618 cm^{-1} and a multiplet of peaks at 3681, 3695, and 3703 cm^{-1}. The frequencies of the symmetric and antisymmetric O–H stretches of water at 3657 and 3756 cm^{-1} are shown as red dashed vertical lines in this figure.[88] The two bands seen for each of the rare gas complexes are therefore at frequencies 20–60 cm^{-1} lower than the two water vibrations. Following assignment patterns seen previously for other metal ion–water complexes,[77] we associate the two bands in each of these complexes with the symmetric and antisymmetric O–H stretches of water, which are shifted to lower frequencies by the binding to the metal cation. As we have discussed in a recent review,[77] such a red shift has been seen for many other metal cation–water complexes and associated with the charge transfer interaction in these systems. Bonding electron density in the water orbitals is polarized toward the metal ion, reducing the bond strengths and consequently reducing the frequencies of the O–H stretches. Another aspect of the charge transfer is that the bands associated with the symmetric and antisymmetric stretching vibrations have roughly equal intensities, in contrast to the much greater intensity seen for the antisymmetric stretch of water itself. The behavior here is similar to that seen for many other cation–water complexes.

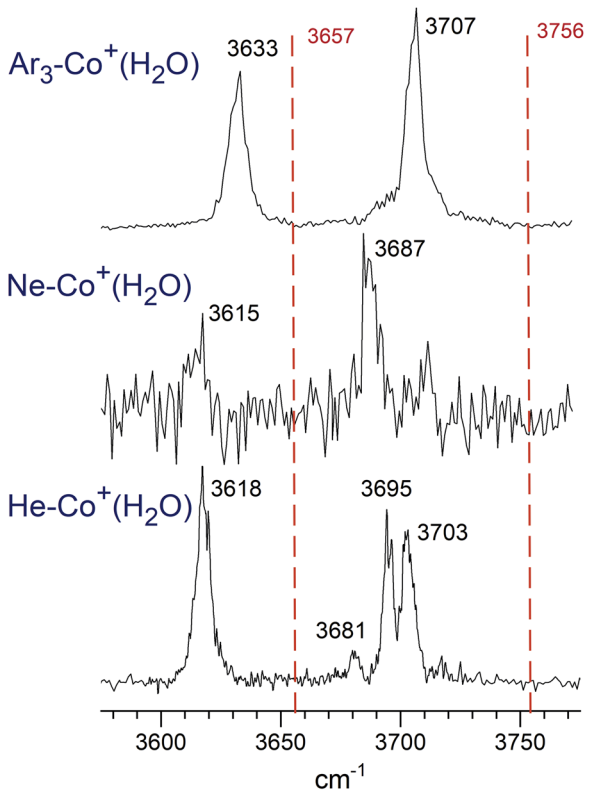

FIG. 1. The photodissociation spectra of $Co^+(H_2O)$ tagged with Ar_3, Ne, and He in the OH stretching region.

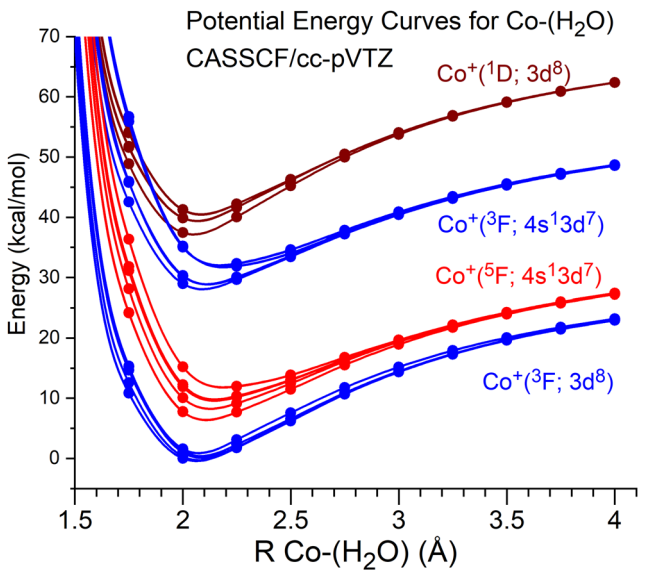

FIG. 2. CASSCF/cc-pVTZ potential energy curves for the approach of a water molecule to the lowest four electronic states of Co^+ in the C_{2v} point group.

Published under license by AIP Publishing

Structures, energetics, and spectra from theory

It is clear that the rare gas binding energies of these complexes would be useful to know to explain their dissociation behavior. Likewise, the differences in the spectra, including the details of vibrational band shifts, also require explanation. We have therefore conducted extensive computational studies on these complexes to investigate their structures, energetics, and spectra. Initially, we constructed the potential energy curves (PECs) for the approach of a water molecule to Co^+ in its first four electronic states. As shown in Fig. 2, the PECs indicate that the lowest energy states of the complex originate from the ground state of $Co^+(^3F; 3d^8)$. We then optimized the first triplet state of each irreducible representation of C_{2v} ($^3A_1$, $^3A_2$, $^3B_1$, $^3B_2$) and the lowest quintet state ($^5B_2$) to make sure that the optimization did not change the energy order of triplets and quintets. The CASSCF wavefunctions for these states showed high single reference character, which then allowed us to perform the geometry optimizations at the more accurate CCSD(T) levels of theory, using MOLPRO.[85] The resulting optimized geometrical parameters (R distances in Å and θ angle in degrees) along with the dominant electronic configuration and the relative energy (ΔE in cm^{-1}) of these five states are presented in Table I. The order of lowest energy

TABLE I. Geometric parameters and relative energies of $Co^+(H_2O)$, He–$Co^+(H_2O)$, Ne–$Co^+(H_2O)$, and Ar_3–$Co^+(H_2O)$ predicted by theory at the CCSD(T)/cc-pVTZ level except where indicated for MN15/cc-pVTZ. The orbitals corresponding to the indicated configurations are shown in Fig. S7 in the supplementary material.

$Co^+(H_2O)$					
State	R(Co–O)	R(O–H)	θ(H–O–H)	ΔE (cm^{-1})	Configuration
$^3B_1$	1.975	0.964	106.6	+0.0	$\sigma_s^0\pi_x^1\pi_y^2\sigma_d^2\delta_+^1\delta_-^2$
$^3A_2$	2.003	0.963	106.6	+17.9	$\sigma_s^0\pi_x^2\pi_y^2\sigma_d^1\delta_+^2\delta_-^1$
$^3A_1$	2.004	0.963	106.6	+31.6	$\sigma_s^0\pi_x^2\pi_y^2\sigma_d^1\delta_+^1\delta_-^2$
$^3B_2$	2.013	0.963	106.8	+711	$\sigma_s^0\pi_x^2\pi_y^1\sigma_d^2\delta_+^1\delta_-^2$
$^5B_2$	2.052	0.967	106.8	+5321	$\sigma_s^1\pi_x^1\pi_y^2\sigma_d^1\delta_+^2\delta_-^1$
$^3B_1$[b]	1.936	0.967	108.9		
He-$Co^+(H_2O)$					
State	R(Co–O)	R(O–H)	θ(H–O–H)	R(Co–He)	ΔE (cm^{-1})
$^3A_2$	1.987	0.963	106.8	1.801	+0.0
$^3A_1$	1.987	0.963	106.8	1.801	+14.6
$^3B_1$	1.953	0.964	106.8	1.882	+348.8
$^3B_2$	1.990	0.963	107.0	1.884	+1075.6
$^3B_1$[b]	1.922	0.967	109.1	1.849	
Ne-$Co^+(H_2O)$					
State	R(Co–O)	R(O–H)	θ(H–O–H)	R(Co-Ne)	ΔE (cm^{-1})
$^3B_1$	1.960	0.964	106.8	2.320	+0.0
$^3A_2$	1.998	0.963	106.7	2.345	+95.5
$^3A_1$	1.998	0.963	106.6	2.349	+110.0
$^3B_2$	1.998	0.963	107.0	2.326	+730.1
$^3B_1$[b]	1.927	0.967	109.0	2.260	
Ar_3-$Co^+(H_2O)$					
State	R(Co–O)	R(O–H)	θ(H–O–H)	R(Co-Ar)	R(Co-Ar')[a]	ΔE (cm^{-1})
$^3A_1$	2.041	0.962	106.4	2.490	2.701	+0.0
$^3A_2$	2.030	0.962	106.5	2.467	2.769	+406.8
$^3B_1$	2.040	0.962	106.7	2.468	2.719	+596.8
$^3B_2$	1.958	0.963	106.9	2.379	3.488	+1043.5
$^3B_1$[b,c]	1.968	0.966	108.9	2.452	2.578	

[a]Ar′ indicates the two argon atoms that are not in the HOH plane; the Ar′CoO angles are 91.5°, 92.2°, 91.7°, and 99.1° for $^3A_1$, $^3A_2$, $^3B_1$, and $^3B_2$, respectively.
[b]Computed with MN15/cc-pVTZ.
[c]Ar′CoO angle is 93.6°.

Published under license by AIP Publishing

TABLE II. Computed energies and ligand binding energies for RG–Co^+, $Co^+(H_2O)$, and RG–$Co^+(H_2O)$ complexes (kcal/mol and cm^{-1} in parentheses; zero-point corrected). The binding energies for tag-free complexes are for the elimination of water; for all others, it is the energy required to eliminate one rare gas atom from the complex.

Ion	ZPVE corrected E. (h)	Binding energy MN15/cc-pVTZ	Binding energy CCSD(T)/cc-pVTZ
Co^+He	−1 385.568 242	4.3 (1 500)	
Co^+Ne	−1 511.528 490	5.4 (1 890)	
Co^+Ar	−1 910.122 236	13.4 (4 690)	
$Co^+(H_2O)$	−1 459.075 256	47.4 (16 580)	
$Co^+(D_2O)$	−1 459.081 597	47.7 (16 680)	
$He–Co^+(H_2O)$	−1 461.999 877	3.5 (1 220)	2.94[a] (1030)
$He–Co^+(D_2O)$	−1 462.006 225	3.5 (1 220)	
$Ne–Co^+(H_2O)$	−1 587.959 693	4.3 (1 500)	2.95[a] (1030)
$Ar–Co^+(H_2O)$	−1 986.553 665	12.4 (4 340)	
$Ar_2–Co^+(H_2O)$	−2 514.023 756	7.2 (2 520)	
$Ar_3–Co^+(H_2O)$	−3 041.476 646	1.8 (630)	4.86[b] (1700)

[a]Zero-point correction using CCSD/cc-pVTZ frequencies.
[b]Zero-point correction using MN15/cc-pVTZ frequencies. This value is the average of the three bonds.

state to the highest was found to be $^3B_1$, $^3A_2$, $^3A_1$, and $^3B_2$. The three lowest states were found to be within 32 cm^{-1} of each other. Both the relative energies and geometric parameters computed here for $Co^+(H_2O)$ are in close agreement with the values reported by Metz and co-workers using CCSD(T) computations.[50] The $^5B_2$ state is confirmed to lie higher in energy.

To validate the energetics of our MN15 computations, we compared them with our CCSD(T) results on selected complexes [$He–Co^+(H_2O)$, $Ne–Co^+(H_2O)$, and $Ar_3–Co^+(H_2O)$], with zero point corrections using CCSD frequencies. As shown in the supplementary material, the structures obtained with MN15 and CCSD(T) are similar. The Co^+–RG and Co^+–RG bond lengths are systematically shorter with MN15 by up to 0.07 Å. The MN15 O–H bond lengths are all within 0.004 Å of those computed with CCSD(T), although the HOH bond angles predicted by MN15 are consistently 2° larger. Likewise, as shown in Table II, the binding energies vary only slightly between the two methods, establishing that the structures and energetics obtained with MN15 are reasonably reliable. Co^+–RG bond energies are found to be consistently greater when calculated with MN15. $He–Co^+(H_2O)$ and $Ne–Co^+(H_2O)$ are found to have C_{2v} structures at both the CCSD(T) and MN15 levels of theory, and $Ar–Co^+(H_2O)$ is found to have the same symmetry with MN15. $Ar_2–Co^+(H_2O)$ (MN15) and $Ar_3–Co^+(H_2O)$ [MN15 and CCSD(T)], each have two argon atoms located in a plane perpendicular to the $Co^+–H_2O$ plane; $Ar_3–Co^+(H_2O)$ has a third argon above this plane and in the same plane as the $Co^+–H_2O$. Table I lists the structural parameters determined for all these complexes. Figure 3 shows a summary of the key aspects of the structures of these complexes, using geometries determined from the complete set of data at the MN15 level.

As shown in Fig. 3, all of the RG–$Co^+(H_2O)$ complexes retain the basic structure of the core $Co^+(H_2O)$ ion, whose bond distances

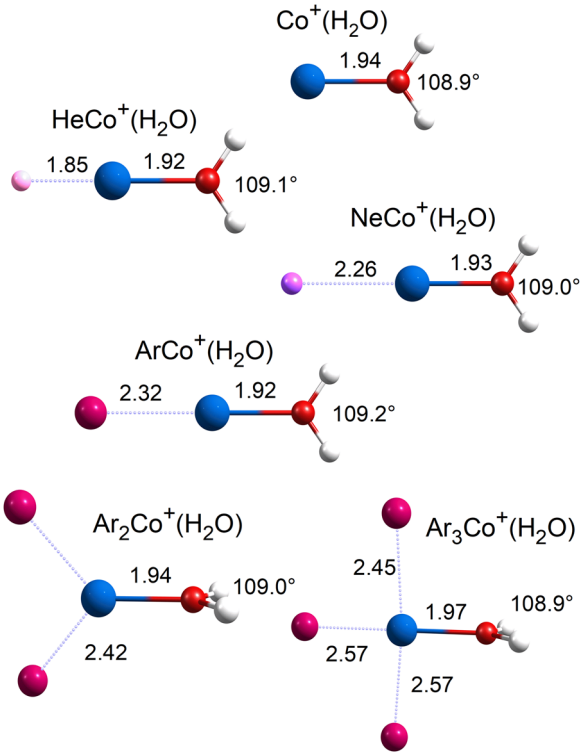

FIG. 3. Structures determined by theory for the tag-free and tagged complexes of $Co^+(H_2O)$ at the MN15/cc-pVTZ level. These calculations were not symmetry restricted and the $Co^+(H_2O)$, $Ar–Co^+(H_2O)$, $Ne–Co^+(H_2O)$, and $He–Co^+(H_2O)$ each converged to $^3B_1$ electronic states. The $Ar_2–Co^+(H_2O)$ and $Ar_3–Co^+(H_2O)$ complexes converged to $^3B_2$ states.

Published under license by AIP Publishing

and H–O–H bond angles vary only slightly with the addition of different rare gas atoms. The structures shown here for the di- and tri-argon complexes are the most stable, but as shown in the supplementary material, there are other isomers with argon atoms attached to the OH of water. The 1.94 Å Co^+–OH_2 bond distance in the tag-free complex decreases very slightly to 1.92 Å in the singly tagged complexes of each of the rare gas atoms, which have the rare gas bonded opposite the water in a complex with overall C_{2v} symmetry. The Co^+–OH_2 bond distance is also found to decrease upon attachment of He or Ne with CCSD(T) within the $^3B_1$ electronic state by 0.022 and 0.015 Å, respectively. However, CCSD(T) predicts a $^3A_2$ ground state for He–$Co^+(H_2O)$ to be 348.8 cm^{-1} lower in energy, which has a 0.034 Å longer Co^+–OH_2 bond distance than the $^3B_1$ state. The trend is reversed in the di- and tri-argon complexes, which have the same and an even longer bond distance, respectively, as the tag-free complex. Presumably, this is because of the more symmetric ligand environment around the cobalt ion, which reduces the polarization along the C_2 axis. Even a minimal charge delocalization among the argon atoms results in a reduced charge on the cobalt ion and a weaker polarizing effect on the water. MN15 NBO calculations predict a natural charge of 0.936 on Co^+ for $Co^+(H_2O)$ and 0.549 for Ar_3–$Co^+(H_2O)$, though this effect may be overestimated by MN15 that yields RG–Co^+ bond energies larger than those predicted by CCSD(T). The bond distance change is related to the change in the H–O–H bonding angle. In the tag-free complex, this angle is 108.9°, which is expanded from the corresponding angle in the isolated water molecule (104.5°). This angle expansion has been reported previously for many cation–water complexes, and attributed to the polarization of the lone-pair electron density of water toward the metal.[77] This effect is also enhanced slightly in the singly tagged complexes which each have an H–O–H angle of 109.1°, but it is relaxed again to smaller values more like the tag-free complex in the di- and tri-argon complexes. However, all of these structural variations induced by the rare gases are quite small and do not change the qualitative structure of the $Co^+(H_2O)$ ion.

The binding energies of these ion complexes help to explain their photodissociation behavior. The calculated MN15 energetics of Co^+–RG, $Co^+(H_2O)$, $Co^+(D_2O)$, RG–$Co^+(H_2O)$, and RG–$Co^+(D_2O)$ are presented in Table II. For comparison, selected complexes were done also at the CCSD(T) level. The bond dissociation energies are those for the elimination of water in the tag-free ions, and for the elimination of one rare gas atom in the tagged complexes. The tendency of DFT to overestimate binding energies is illustrated in the binding energies of Co^+Ne and Co^+Ar, whose computed values of 5.4 and 13.4 kcal/mol can be compared to the experimentally determined values 2.7[82] and 12.8[79] kcal/mol, respectively. The strong bonds found in these Co^+–RG complexes are a result of the small ionic radius of cobalt, and the resulting polarizing effect of the more concentrated charge. Likewise, the binding energy of 47.4 kcal/mol computed for $Co^+(H_2O)$ can be compared to its experimental values of 39–40 kcal/mol.[4–6] Where comparisons are possible for He–$Co^+(H_2O)$ and Ne–$Co^+(H_2O)$, the MN15 results are systematically higher than the CCSD(T) results. Therefore, the MN15 binding energies computed should be considered overestimated by a few kcal/mol, but they do provide some guidance in these experiments. The helium and neon binding energies in these complexes are comparable; apparently, the larger Ne–Co^+ distance compensates for the polarizability difference. This effect has been discussed previously in computational studies of RG–Co^+ complexes.[80,81] Our failure to photodissociate Ar–$Co^+(H_2O)$ in the O–H stretching region is consistent with the high binding energy predicted. Our ability to dissociate He–$Co^+(H_2O)$ and Ar_3–$Co^+(H_2O)$ is consistent with their low predicted binding energies. However, our failure to dissociate Ne–$Co^+(H_2O)$ and Ar_2–$Co^+(H_2O)$ seem to be caused by issues other than dissociation energies. In these cases, parent ion densities seem to be adequate, and therefore, the dissociation *rate* may be the source of these difficulties. This rate depends not only on the bond energy but also on the efficiency of intramolecular vibrational redistribution (IVR) from the O–H stretches excited initially to the RG–Co^+ dissociation coordinate.

The frequencies predicted by theory for the vibrations of the various RG–$Co^+(H_2O)$ complexes allow the spectral trends in Fig. 1 to be investigated. Figure 4 shows the predicted positions of the water scissors bend and O–H stretching modes for the tag-free $Co^+(H_2O)$ complex and those tagged with Ar_3, Ne, and He. The

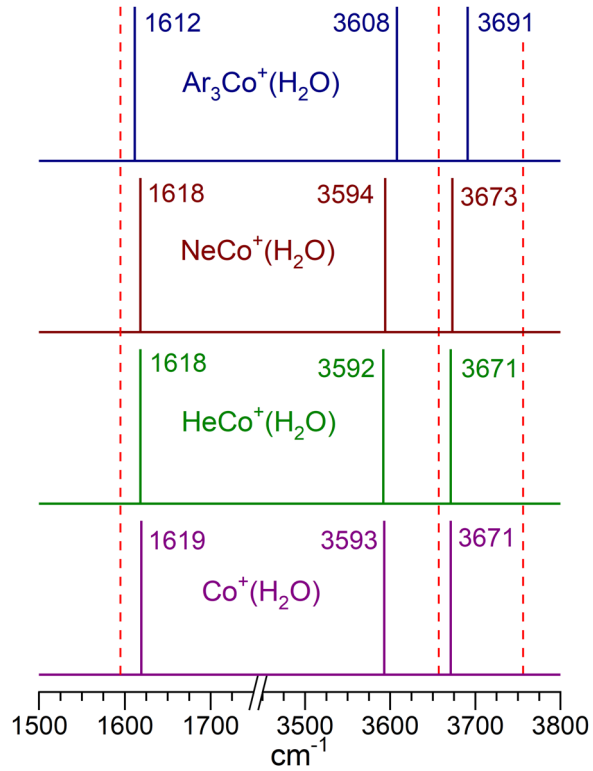

FIG. 4. Stick spectra showing the predicted positions of H_2O vibrational transitions for tag-free $Co^+(H_2O)$ and for this ion tagged with Ar_3, Ne, or He, based on scaled harmonic computations at the MN15/cc-pVTZ level. These calculations were not symmetry restricted and arrived at the $^3B_1$, $^3B_2$, $^3B_1$, and $^3B_1$ electronic states, respectively. The positions of these transitions are nearly unchanged for tagging with Ne or He. The red dashed lines show the positions of the experimental frequencies for these vibrations in the isolated water molecule (bending mode at 1595 cm^{-1}; O–H stretches at 3657 and 3756 cm^{-1}, respectively).

Published under license by AIP Publishing

Ar_3 complex data here are for the most stable structure, which has all three argon atoms attached to the cobalt ion. As shown in Fig. S19 in the supplementary material, this is the structure whose predicted band patterns agree with our measured spectrum. The frequency shifts expected for mono- and di-argon complexes are presented in Figs. S17 and S18. The frequencies determined here for the tag-free complex at the DFT/MN15 level of theory are in reasonably good agreement with those reported by Metz and coworkers at the DFT/BHandHLYP level.[50] Our frequencies for the OH stretches are within 11 cm^{-1} of those predicted by Metz. However, the H–O–H scissors bend predicted by Metz is 36 cm^{-1} lower than our value. All of the O–H stretches predicted by our calculations are shifted to frequencies lower than those of the isolated water molecule, consistent with the experiment. In addition, consistent with the experiment, the bands of the Ar_3–$Co^+(H_2O)$ complex appear at higher frequencies than those of the other complexes, indicating a smaller red-shift from the frequencies of the isolated water molecule. This may be caused by a slightly lower effective charge of the cobalt ion caused by delocalization of charge among the argon ligands, leading to less polarization of the water. Consistent with this idea, the Co^+–O bond distance for the $Ar_3Co^+(H_2O)$ complex is longer than it is for the other complexes (1.97 vs 1.92–1.93 Å). Likewise, the Ar_3 complex has a bending mode that is less shifted than those of the other complexes. In both the O–H stretching region and the H–O–H bending region, the band positions of the tag-free complex and those tagged with He or Ne are all within 2 cm^{-1} of each other. This shows that the smaller rare gases contribute vanishingly small perturbations to the vibrational structure of the molecule. Rare gas tagging is usually employed with the hope that the frequencies of the tagged complex are nearly the same as those of the tag-free complex. This is apparently a good approximation for both He–$Co^+(H_2O)$ and Ne–$Co^+(H_2O)$, but not for Ar_3–$Co^+(H_2O)$.

Spectra of helium tagged $Co^+(H_2O)$ and $Co^+(D_2O)$

Because helium and neon are now established as inert tags, and because the binding energy of helium to $Co^+(H_2O)$ is quite low, helium tagging should be useful to investigate a wider range of the spectrum of this ion. We, therefore, used this to measure spectra in the lower frequency region for He–$Co^+(H_2O)$ and to do the same for the deuterated He–$Co^+(D_2O)$ complex. The spectra measured for these ions are shown in Fig. 5. Single peaks are observed for the H_2O bend and symmetric stretch, whereas the multiplet structure is seen in the region of the antisymmetric stretch, as shown in more detail in Fig. 1. Both the symmetric and antisymmetric O–H stretches are shifted about 60 cm^{-1} lower than the frequencies of these vibrations in the isolated water molecule due to the interaction with Co^+. The H_2O scissors bend vibration at 1618 cm^{-1} is shifted 23 cm^{-1} to higher frequency from this interaction. This vibration has not been accessible in previous studies of metal ion–water complexes. Apparently, the ligand polarization that opens the H–O–H bond angle affects the potential in such a way so as to make the bending motion slightly more rigid. Like the O–H stretches, the D_2O O–D stretches experience a red shift from the interaction with Co^+. The symmetric and antisymmetric stretches of the He–$Co^+(D_2O)$ complex at 2638 and 2743 cm^{-1} are comparable to the vibrations at 2671 and 2788 cm^{-1} for D_2O, respectively.[88] No D_2O bend was

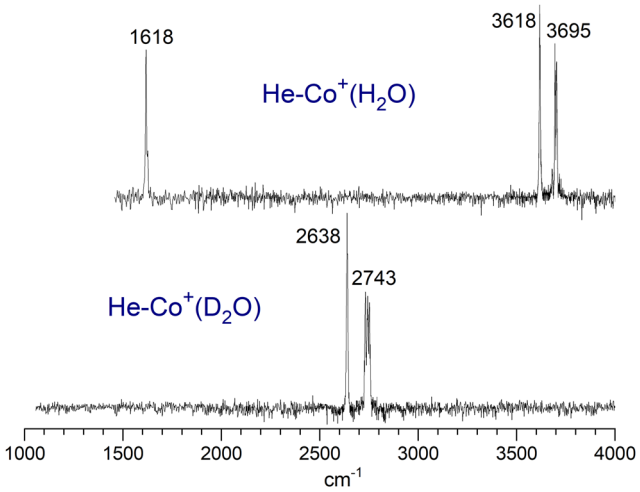

FIG. 5. Infrared photodissociation spectra of He–$Co^+(H_2O)$ and He–$Co^+(D_2O)$.

detected, presumably because of either a low fragmentation yield or the lower laser power available in this region of the spectrum. The bend vibration of isolated D_2O occurs at 1178 cm^{-1},[88] which is close to the predicted dissociation threshold for the elimination of helium from He–$Co^+(D_2O)$, and this vibration in the $Co^+(D_2O)$ complex would be expected at slightly higher energy than this if the interaction is like that of $Co^+(H_2O)$.

Further details of the symmetric and antisymmetric stretch bands of He–$Co^+(H_2O)$ are shown in Fig. 6. By comparison with the spectra of many other metal cation–water complexes,[58,60,66,75–77] we can conclude that these bands have partially resolved rotational structure. The symmetric stretch and bending modes are parallel-type vibrational bands, whose contours are dominated by overlapping $\Delta K = 0$ subbands (i.e., $K'' = 0 \rightarrow K' = 0$, $K'' = 1 \rightarrow K' = 1$, etc.). The $K'' = 0$ and 1 levels both survive down to the lowest temperatures because of their respective nuclear spin symmetries. The antisymmetric stretch is a perpendicular-type band with more widely spaced multiplet structure caused by the large value of the *A* rotational constant, which corresponds to rotational motion involving primarily the light hydrogen atoms moving around the C_2 axis. Three $\Delta K = \pm 1$ subbands are prominent at low temperature corresponding to the $K'' = 0 \rightarrow K' = 1$, $K'' = 1 \rightarrow K' = 0$, and $K'' = 1 \rightarrow K' = 2$ transitions. We use the spectroscopic program PGopher[89] to simulate this rotational structure for two possible kinds of electronic states in the lower two traces in the figure. Because the *B* and *C* rotational constants are nearly equivalent and much smaller than our resolution, these simulations are done with a prolate symmetric-top approximation. The band origin and *A* rotational constant are adjusted in the simulation to match the appearance of the spectrum; the *B* and *C* constants are taken from theory. The simulation includes the 3:1 (or 1:3) nuclear spin weighting for K'' states of the fermionic hydrogens, which varies with the electronic state symmetry. If the electronic ground state is symmetric (i.e., the $^3A_2$ or $^3A_1$), there is a 1:3 degeneracy factor applied to even:odd values of K'', and the transitions originating in the

Published under license by AIP Publishing

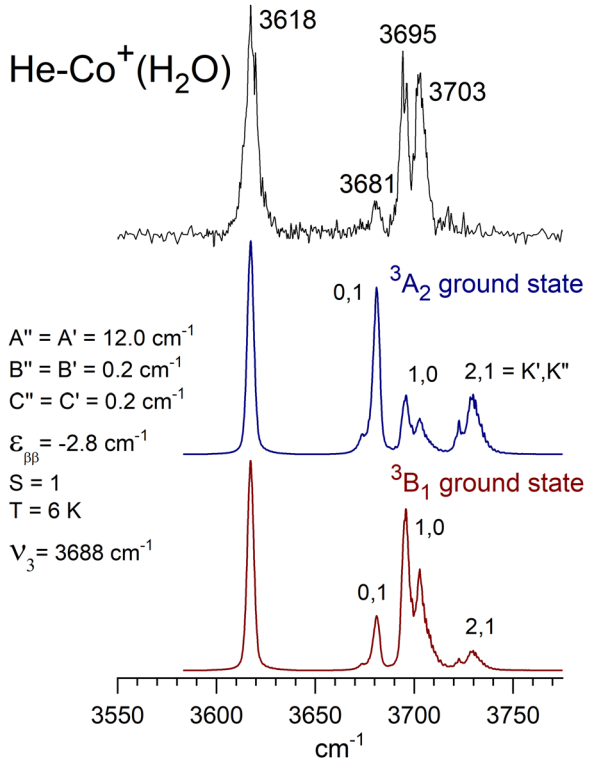

FIG. 6. The measured spectrum of He–$Co^+(H_2O)$ in the O–H stretching region (upper trace) compared to pGopher simulations of the spectrum for two possible electronic states.

K″ = 1 level (those split away from the center of the spectrum) are more intense. If the electronic ground state is antisymmetric (i.e., $^3B_1$ or $^3B_2$), the degeneracy switches to 3:1 for even:odd K″ states, and the transitions originating in K″ = 0 near the center of the spectrum are more intense. Additional details about this kind of rotational structure are given in Ref. 50. The simulation also includes the spin-rotation interaction, which introduces an additional small splitting to transitions originating in K″ = 0. As shown previously by Metz and co-workers, it is necessary to explain the multiplet structure seen for $Co^+(H_2O)$,[50] and we find it necessary to include here as well. A spin-rotation interaction was also necessary to explain the spectrum of $Ti^+(H_2O)$ measured previously by our group.[75] The various constants determined from these rotational simulations are shown in the figure.

As shown, the experimental spectrum matches the pattern predicted for an antisymmetric electronic state quite nicely. The rotational temperature of 6 K is consistent with the expectations for an ion that is cold enough to form a helium complex. Our calculations predict that He–$Co^+(H_2O)$ has low-lying $^3A_2$, $^3A_1$, and $^3B_1$ states, with a $^3B_2$ state lying much higher in energy, and, therefore, excluded from consideration. The rotational structure in this spectrum is inconsistent with that predicted for the $^3A_2$ or $^3A_1$ states and, therefore, indicates that the ground state is the antisymmetric $^3B_1$ state. The $^3B_1$ state was found experimentally to be the ground state for the tag-free $Co^+(H_2O)$ complex by Metz and co-workers,[50] and this state was also found as the ground state by our theory and that of Metz[50] for the tag-free complex. However, our CCSD(T) results predict a $^3A_2$ or $^3A_1$ ground state for the helium complex. Higher electron correlation effects may be necessary for these systems. However, selected computations with larger basis sets did not change the state ordering. Because the $^3B_1$ state is the ground state for the tag-free complex, it is conceivable that during He attachment, the $^3B_1$ state is conserved, and survives as a metastable excited state, simply because the system has not relaxed to the $^3A_2$ ground state. Metastable states can be formed and can survive in experiments like these, and there are examples of this in the literature.[90] However, in this case, it is difficult to see what could trap the $^3B_1$ state. The spin of both states is the same, so there is no spin-forbidden transition. The geometry is essentially the same, so there is not likely to be any barrier to go from one to the other. The only difference is the orbital occupation, and it seems that the system would naturally choose the lower energy configuration.

Figure 7 shows a similar expanded view of the partially resolved rotational structure for the antisymmetric stretch of the He–$Co^+(D_2O)$ complex compared to the same kind of rotational simulations. In this case, not only is the rotational constant smaller, but the nuclear spin statistical weighting changes because D is a boson. If the electronic ground state is symmetric (i.e., $^3A_2$ or $^3A_1$),

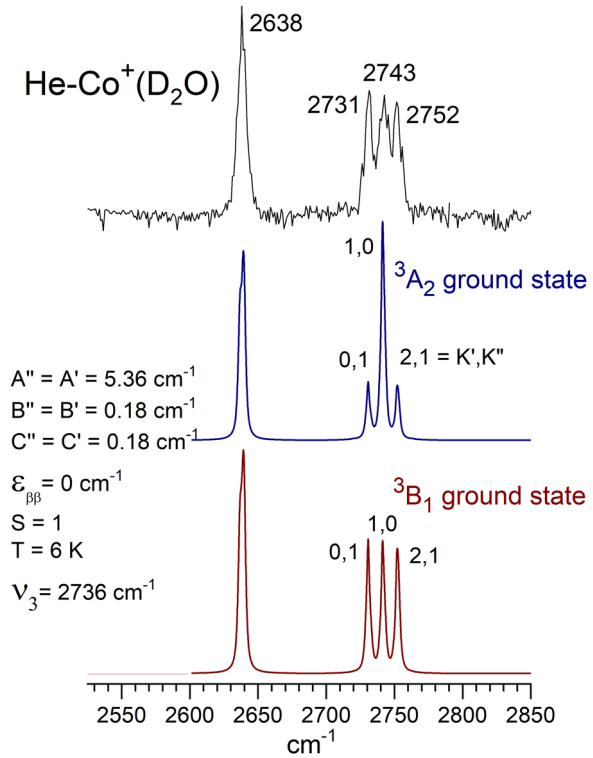

FIG. 7. The measured spectrum of He–$Co^+(D_2O)$ in the O–D stretching region (upper trace) compared to pGopher simulations of the spectrum for two possible electronic states.

Published under license by AIP Publishing

there is a 2:1 degeneracy factor applied to even:odd values of K″, and the transitions originating in the K″ = 0 level (those near the center of the spectrum) are more intense. If the electronic ground state is antisymmetric (i.e., $^3B_1$ or $^3B_2$), the degeneracy switches to 1:2 for even:odd K″ states, and the transitions originating in K″ = 1 away from the center of the spectrum are enhanced. As shown, the patterns expected are significantly different for the symmetric vs antisymmetric electronic ground state, and again, the experimental pattern matches with that for the antisymmetric $^3B_1$ state. The rotational structure in both He–$Co^+(H_2O)$ and He–$Co^+(D_2O)$ therefore confirms that the ground state of these complexes is the $^3B_1$ state.

Having assigned the rotational structure, we can determine the band origins for the symmetric and antisymmetric stretches to within the accuracy of our spectral linewidths. The experimental linewidths (5–7 cm^{-1}) are larger than the laser linewidth (2 cm^{-1}) and are determined by a combination of unresolved ΔJ transitions determined by the temperature of the experiment, as well as any contribution from predissociation. The symmetric and antisymmetric stretches of He–$Co^+(H_2O)$ are, therefore, 3618 and 3688 cm^{-1}, respectively, whereas those for He–$Co^+(D_2O)$ are 2638 and 2736 cm^{-1}. The He–$Co^+(H_2O)$ values can be compared to the frequencies determined by Metz and co-workers in an IR-optical double resonance experiment on the tag-free $Co^+(H_2O)$ ion.[50] The symmetric stretch reported in that experiment was 3610 cm^{-1} and the antisymmetric stretch band origin was 3680 cm^{-1}. The K′, K″ = 1,0 subband position for the tag-free complex was 3693 cm^{-1}, compared to our value of 3695 cm^{-1}. The very slight disagreement between the tag-free and helium-tagged band positions are likely caused by the different temperatures/linewidths in the two experiments (~5 cm^{-1} for our 6 K spectra; 10–12 cm^{-1} for Metz at 15 K). Another possible issue affecting the exact band origin is the different spin-rotation constants used in the two experiments (see below). However, it is clear that the helium induces an extremely small shift, if any, to these vibrational frequencies.

An interesting aspect of these spectra is the values of the rotational constants suggested by the simulations. The *A* constants are determined accurately by the main spacings in the spectra for the antisymmetric stretch and have the values of 12.0 and 5.36 cm^{-1} for He–$Co^+(H_2O)$ and He–$Co^+(D_2O)$, respectively. In both cases, these values are significantly lower than those for the corresponding H_2O and D_2O molecules (14.5 and 7.27 cm^{-1})[88] and also lower than the values predicted by theory for the He–$Co^+(H_2O)$ and He–$Co^+(D_2O)$ complexes [Table III; 13.96 and 6.98 cm^{-1} at the CCSD(T) level]. The He–$Co^+(H_2O)$ and He–$Co^+(D_2O)$ constants determined here are also lower than those obtained by Metz and co-workers for the tag-free $Co^+(H_2O)$ and $Co^+(D_2O)$ ions (13.74 and 6.87 cm^{-1}).[50] Apparently, the presence of the helium changes (reduces) the rotational constants. The constants derived from theory are for the equilibrium structures, which have the helium in a position opposite the water and on the C_2 symmetry axis. In this position, the helium should not affect the *A* constant. Consistent with this, the values from theory are virtually identical for the tag-free or helium-tagged ion. The helium can affect the rotational constant only if it is located off the C_2 axis. Bent equilibrium structures are ruled out by the consistent computational results from different levels of theory. The only remaining possibility is *dynamical* bending, i.e., through vibrational averaging involving the bending modes. If the helium atom position is slightly off-axis on average because of such bending, this would lower the *A* rotational constant. This effect has been suggested in previous work on singly tagged RG–$M^+(H_2O)$ complexes.[76] Table III shows the results of calculations for the rotational constants through a VPT2 treatment of vibrational averaging. As shown, the *A* constants for the He–$Co^+(H_2O)$ and He–$Co^+(D_2O)$ constants are indeed reduced by this effect, although the magnitude of the effect is under-estimated. Nevertheless, this seems to be the best explanation for the smaller-than-expected values of the *A* rotational constants.

TABLE III. Equilibrium (A_{eq}'', B_{eq}'', and C_{eq}'') and vibrationally averaged (A_0'', B_0'', and C_0'') rotational constants. Vibrational averaged values were derived from anharmonic computations at the MN15/cc-pVTZ level using VPT2 in Gaussian 16.

CCSD(T)/cc-pVTZ Ion	A_{eq}''	B_{eq}''	C_{eq}''			
He–$Co^+(H_2O)$ $^3A_2$	14.00	0.21	0.21			
He–$Co^+(H_2O)$ $^3A_1$	14.00	0.21	0.21			
He–$Co^+(H_2O)$ $^3B_1$	13.96	0.22	0.21			
He–$Co^+(D_2O)$ $^3A_2$	7.01	0.19	0.19			
He–$Co^+(D_2O)$ $^3A_1$	7.01	0.19	0.19			
He–$Co^+(D_2O)$ $^3B_1$	6.98	0.19	0.19			
MN15/cc-pVTZ Ion	A_{eq}''	B_{eq}''	C_{eq}''	A_0''	B_0''	C_0''
$Co^+(H_2O)$ $^3B_1$	13.50	0.30	0.30	13.36	0.30	0.29
$Co^+(D_2O)$ $^3B_1$	6.76	0.26	0.25	6.71	0.26	0.25
He–$Co^+(H_2O)$ $^3B_1$	13.47	0.22	0.22	12.58	0.22	0.22
He–$Co^+(D_2O)$ $^3B_1$	6.74	0.20	0.19	6.51	0.20	0.19
Ne–$Co^+(H_2O)$ $^3B_1$	13.49	0.10	0.10	11.91	0.10	0.09
Ar–$Co^+(H_2O)$ $^3B_1$	13.47	0.06	0.06	12.86	0.06	0.06
Ar_2–$Co^+(H_2O)$ $^3B_2$	0.07	0.06	0.03	0.07	0.06	0.03
Ar_3–$Co^+(H_2O)$ $^3B_2$	0.06	0.03	0.02	0.06	0.03	0.02

Another more subtle effect in these spectra is the splitting induced by spin-rotation coupling, which results from the interaction of both orbital and electron spin angular momenta with the rotational angular momentum. As shown in Fig. 6, the simulation for the $^3B_1$ ground state matches the experimental spectrum for He–$Co^+(H_2O)$ nicely, including the splitting that gives rise to the 3695/3703 cm^{-1} doublet. This doublet arises from the spin-rotation interaction, and is determined by the magnitude of the spin-rotation coupling constant, ε. Epsilon is a tensor with different components, and we find that the $\varepsilon_{\beta\beta}$ component is the only one that allows us to match our spectrum. Without the inclusion of this interaction for He–$Co^+(H_2O)$, we cannot reproduce the experimental pattern. On the other hand, we find that the inclusion of this constant destroys the agreement between the simulation and the experiment for the He–$Co^+(D_2O)$ complex. The same kind of spin-rotation interaction produced prominent doublets in the spectrum of $Ti^+(H_2O)$,[75] and indeed, Metz and co-workers included

Published under license by AIP Publishing

this in their simulations of the rotational structure of the tag-free $Co^+(H_2O)$ ion.[50] The spin-rotation coupling constant employed by Metz to explain their spectrum for $Co^+(H_2O)$ (-6 cm^{-1}) was much larger than the value used here (-2.8 cm^{-1}), and they used the different $\varepsilon_{\alpha\alpha}$ component of this. However, the resolution in the Metz experiment was limited so that the constant does not appear to be highly determined. Metz although also found a much smaller constant for the D_2O complex than they did for the H_2O complex. It is therefore not clear whether or not the addition of helium in our experiment has a significant effect on the spin-rotation interaction.

A final aspect of these spectra is that the rotational patterns are described well by employing the normal nuclear spin statistical weighting expected for a system with identical H (or D) atoms. This is consistent with our findings for several other transition metal ion–water complexes studied previously[60,66,67,75] but is in contrast with our recent results for the argon- and neon-tagged vanadium and niobium cation–water complexes.[76] In the latter systems, ortho–para interconversion took place depending on the symmetry of the ground electronic states, eliminating the usual alternating line intensities resulting from nuclear spin statistics. This was interpreted to arise from a nuclear spin coupling with the hydrogen atoms through a large Fermi contact interaction. To explore this effect in the present system in which such ortho–para interconversion apparently does not occur, we employed CCSD/cc-pVTZ computations to calculate the isotropic Fermi contact interaction for $Co^+(H_2O)$. The Fermi contact term A_K was found to vary between zero and -1 MHz for all electronic states with both hydrogen and deuterium. These values are significantly smaller than those found for vanadium and niobium cations ($A_K = 2$–4 MHz), consistent with the lack of ortho–para interconversion in the present cobalt cation complexes.

From these various data on the spectra of $Co^+(H_2O)$ with different tag atoms, we can make some general conclusions about the effects of these tag atoms on the structure and spectroscopy of metal cation complexes. First, these computations at the reliable CCSD(T) level of theory, complemented by DFT/MN15 computations, show that the binding energies of the rare gas atoms to Co^+ are quite substantial. The helium and neon binding energies are comparable, with values near 3 kcal/mol, whereas the argon binding energy is much greater and near 12 kcal/mol. This explains how we are able to photodissociate the helium complex and not the single-argon complex, but the failure to dissociate the neon complex cannot be explained because of the binding energy. Similar energetic patterns are expected for the rare gas complexes of other late transition metal-containing ions. Although the binding energies are substantial, the addition of argon, neon, or helium to the $Co^+(H_2O)$ complex does not change the structure of the core ion in any significant way. In contrast, the vibrational spectra are affected, most substantially by argon. Vibrational shifts are extremely small for the neon or helium complexes. However, all the rare gas vibrational shifts are much smaller than the shifts induced on the water vibrations by binding to the cobalt.

Rotational information is obtained here only for the helium complex. Its analysis confirms the structures of the $He–Co^+(H_2O)$ and $He–Co^+(D_2O)$ complexes and allows the determination of the electronic ground state for these ions. Surprisingly, the ground electronic state predicted by CCSD(T) computations for the helium complex ions does not match with that of the experiment, presumably because the effect of the helium binding on the electronic interaction is slightly overestimated. An interesting surprise is that the helium tag atoms affect the rotational constants of these complexes, reducing them slightly by vibrational averaging of the structures through off-axis bending motion. This effect is likely to be more significant for neon or argon complexes, which have heavier masses in motion. Indeed, several previous examples of $Ar–M^+(H_2O)$ complexes have been studied, which have the same kind of partially resolved rotational structure seen here.[60,66,67,75] In several cases, the measured *A* rotational constant was lower than expected on the basis of theory, and in some cases, this was attributed to larger H–O–H bond angles on the water ligand. In light of the observations here, these previous data may also have been influenced by the effects of rare gas vibrational averaging. It, therefore, seems that rare gas tagging, especially with neon or helium atoms, provides a non-perturbing view of vibrational spectra, but not as clear as a view of the rotational structure. The behavior seen here for metal ion complexes with water can be contrasted to that seen for non-metal protonated ions. In the case of the $(H_2O)H^+(NH_3)$ complex, for example, Johnson and co-workers found that helium tag atoms exhibited "quantum delocalization" and had no significant effect on rotational constants.[91]

CONCLUSIONS

$Co^+(H_2O)$ complexes produced with laser vaporization have been studied with infrared laser spectroscopy using the method of tagging with rare gas atoms. To explore the effects of tagging, complexes with argon, neon, and helium were investigated with photodissociation spectroscopy and computational chemistry at different levels. Computations provide a more complete picture of the spectroscopy than experiments because the experiments are limited by dissociation yields to complexes containing three argon atoms or one helium atom. The spectra of these complexes agree with those predicted by theory, validating the computational methods. Theory finds that the attachment of rare gas atoms to the $Co^+(H_2O)$ ion causes only insignificant changes to the structure of the core ion. Binding energies for single-argon complexes lie above the energies of vibrational fundamentals, whereas those for neon or helium complexes lie below the energies of O–H stretching and bending modes. Although energetically possible, the photodissociation yield of neon complexes is extremely low, prohibiting detailed spectroscopy. The dissociation of helium-tagged complexes is efficient, providing high quality spectra for the O–H stretching and scissors bending vibrations of $Co^+(H_2O)$ as well as the O–D stretches of $Co^+(D_2O)$. The stretching modes of both complexes are shifted to lower frequencies by the metal binding, consistent with trends seen previously for other cation–water complexes. The scissors bending vibration is observed here for the first time and found to shift slightly to higher frequency by the metal binding. The stretch vibrations in the helium-tagged complex are compared to those of the tag-free $Co^+(H_2O)$ complex studied previously and found to have insignificant vibrational shifts induced by the helium. The rotational structures of the antisymmetric stretch vibrational bands for both $He–Co^+(H_2O)$ and $He–Co^+(D_2O)$ are consistent with the same $^3B_1$ ground electronic state found for the tag-free $Co^+(H_2O)$ ion. Theory

Published under license by AIP Publishing

predicts this same ground state for the tag-free ion but finds the $^3A_2$ state to be lower in energy for the helium-tagged ion. The *A* rotational constants found from analysis of the antisymmetric stretch vibration for both He–$Co^+(H_2O)$ and He–$Co^+(D_2O)$ are slightly lower than those for the tag-free complexes, and this is attributed to vibrational averaging caused by the bending of the helium. For $Co^+(H_2O)$ and related cation–water complexes, helium and neon rare gases are concluded to be "inert" with regard to vibrational frequency perturbations, but caution is recommended regarding structural conclusions based on the values of rotational constants.

SUPPLEMENTARY MATERIAL

See the supplementary material for optimized geometries and harmonic frequencies of all computed isomers. Additional figures present infrared spectra of other argon-tagged isomers.

ACKNOWLEDGMENTS

We gratefully acknowledge the generous support for this work from the National Science Foundation (Grant No. CHE-1764111) and the U.S. Department of Energy (Grant No. DE-SC0018835).

DATA AVAILABILITY

The data that support the findings of this study are available within the article (and its supplementary material).

REFERENCES

[1] J. Burgess, *Ions in Solution* (Horwood Publishing, Chichester, UK, 1999).
[2] Y. Marcus, *Ions in Solution and their Solvation* (John Wiley & Sons, Hoboken, NJ, 2015).
[3] P. Kebarle, "Ion thermochemistry and solvation from gas-phase ion equilibria," Annu. Rev. Phys. Chem. **28**, 445 (1977).
[4] T. F. Magnera, D. E. David, and J. Michl, "Gas-phase water and hydroxyl binding-energies for monopositive 1st row transition-metal ions," J. Am. Chem. Soc. **111**, 4100 (1989).
[5] P. J. Marinelli and R. R. Squires, "Sequential solvation of atomic transition-metal ions. The second solvent molecule can bind more strongly than the first," J. Am. Chem. Soc. **111**, 4101 (1989).
[6] N. F. Dalleska, K. Honma, L. S. Sunderlin, and P. B. Armentrout, "Solvation of transition-metal ions by water. Sequential binding energies of $M^+(H_2O)_x$, (x = 1–4) for M = Ti to Cu determined by collision-induced dissociation," J. Am. Chem. Soc. **116**, 3519 (1994).
[7] D. Schröder and H. Schwarz, "Generation, stability, and reactivity of small multiply charged ions in the gas phase," J. Phys. Chem. A **103**, 7385 (1999).
[8] M. Beyer, E. R. Williams, and V. E. Bondybey, "Unimolecular reactions of dihydrated alkaline earth metal dications $M^{2+}(H_2O)_2$, M = Be, Mg, Ca, Sr, and Ba: Salt-bridge mechanism in the proton-transfer reaction $M^{2+}(H_2O)_2 \rightarrow MOH^+ + H_3O^+$," J. Am. Chem. Soc. **121**, 1565 (1999).
[9] L. Poisson, P. Pradel, F. Lepetit, F. Réau, J.-M. Mestdagh, and J.-P. Visticot, "Binding energies of first and second shell water molecules in the $Fe(H_2O)_2^+$, $Co(H_2O)_2^+$ and $Au(H_2O)_2^+$ cluster ions," Eur. Phys. J. D **14**, 89 (2001).
[10] V. E. Bondybey and M. K. Beyer, "How many molecules make a solution?," Int. Rev. Phys. Chem. **21**, 277 (2002).
[11] A. J. Stace, "Metal ion solvation in the gas phase: The quest for higher oxidation states," J. Phys. Chem. A **106**, 7993 (2002).
[12] M. F. Bush, R. J. Saykally, and E. R. Williams, "Formation of hydrated triply charged metal ions from aqueous solutions using nanodrop mass spectrometry," Int. J. Mass Spectrom. **253**, 256 (2006).
[13] M. K. Beyer, "Hydrated metal ions in the gas phase," Mass Spectrom. Rev. **26**, 517 (2007).
[14] T. E. Cooper, D. R. Carl, and P. B. Armentrout, "Hydration energies of zinc (II): Threshold collision-induced dissociation experiments and theoretical studies," J. Phys. Chem. A **113**, 13727 (2009).
[15] D. R. Carl, B. K. Chatterjee, and P. B. Armentrout, "Threshold collision-induced dissociation of $Sr^{2+}(H_2O)_x$ complexes (x = 1–6): An experimental and theoretical investigation of the complete inner shell hydration energies of Sr^{2+}," J. Chem. Phys. **132**, 044303 (2010).
[16] C. van der Linde and M. K. Beyer, "Reactions of $M^+(H_2O)_n$, n<40, M = V, Cr, Mn, Fe, Co, Ni, Cu, and Zn, with D_2O reveal water activation in $Mn^+(H_2O)_n$," J. Phys. Chem. A **116**, 10676 (2012).
[17] C. van der Linde, S. Hemmann, R. F. Höckendorf, O. P. Balaj, and M. K. Beyer, "Reactivity of hydrated monovalent first row transition metal ions $M^+(H_2O)_n$, M = V, Cr, Mn, Fe, Co, Ni, Cu, Zn, towards molecular oxygen, nitrous oxide, and carbon dioxide," J. Phys. Chem. A **117**, 1011 (2013).
[18] P. B. Armentrout, "Fifty years of ion and neutral thermochemistry by mass spectrometry," Int. J. Mass Spectrom. **377**, 54 (2015).
[19] M. T. Rogers and P. B. Armentrout, "Cationic noncovalent interactions: Energetics and periodic trends," Chem. Rev. **116**, 5642 (2016).
[20] T. E. Cooper and P. B. Armentrout, "Threshold collision-induced dissociation of hydrated cadmium (II): Experiment and theoretical investigation of the binding energies for $Cd^{2+}(H_2O)_n$ complexes (n = 4–11)," Chem. Phys. Lett. **486**, 1 (2010).
[21] M. Rosi and C. W. Bauschlicher, "The binding energies of one and two water molecules to the 1st transition-row metal positive ions," J. Chem. Phys. **90**, 7264 (1989).
[22] C. W. Bauschlicher, Jr., M. Sodupe, and H. Partridge, "A theoretical study of the positive and dipositive ions of $M(NH_3)_n$ and $M(H_2O)_n$ for M = Mg, Ca, or Sr," J. Chem. Phys. **96**, 4453 (1992).
[23] A. Ricca and C. W. Bauschlicher, "Successive H_2O binding energies for $Fe(H_2O)_n^+$," J. Phys. Chem. **99**, 9003 (1995).
[24] D. Feller, E. D. Glendening, and W. A. de Jong, "Structures and binding enthalpies of M^+ $(H_2O)_n$ clusters, M = Cu, Ag, Au," J. Chem. Phys. **110**, 1475 (1999).
[25] A. Irigoras, J. E. Fowler, and J. M. Ugalde, "Reactivity of $Sc^+(^3D,^1D)$ and $V^+(^5D,^3F)$: Reaction of Sc^+ and V^+ with water," J. Am. Chem. Soc. **121**, 574 (1999).
[26] A. Irigoras, J. E. Fowler, and J. M. Ugalde, "Reactivity of $Cr^+(^6S,^4D)$, $Mn^+(^7S,^5S)$ and $Fe^+(^6D,^4F)$: Reaction of Cr^+, Mn^+, and Fe^+ with water," J. Am. Chem. Soc. **121**, 8549 (1999).
[27] A. Irigoras, O. Elizalde, I. Silanes, J. E. Fowler, and J. M. Ugalde, "Reactivity of $Co^+(^3F,^5F)$, $Ni^+(^2D,^4F)$, and $Cu^+(^1S,^3D)$: Reaction of Co^+, Ni^+, and Cu^+ with water," J. Am. Chem. Soc. **122**, 114 (2000).
[28] E. C. Lee, H. M. Lee, P. Tarakeshwar, and K. S. Kim, "Structures, energies, and spectra of aqua-silver (I) complexes," J. Chem. Phys. **119**, 7725 (2003).
[29] H. M. Lee, P. Tarakeshwar, J. Park, M. R. Kołaski, Y. J. Yoon, H.-B. Yi, W. Y. Kim, and K. S. Kim, "Insight into the structures, energetics and vibrations of monovalent cation-$(water)_{1-6}$ clusters," J. Phys. Chem. A **108**, 2949 (2004).
[30] H. M. Lee, M. Diefenbach, S. B. Suh, P. Tarakeshwar, and K. S. Kim, "Why the hydration energy of Au^+ is larger for the second water molecule than the first one: Skewed orbitals overlap," J. Chem. Phys. **123**, 074328 (2005).
[31] V. Kasalová, W. D. Allen, H. F. Schaefer III, E. D. Pillai, and M. A. Duncan, "Model systems for probing metal cation hydration: The $V^+(H_2O)$ and $ArV^+(H_2O)$ complexes," J. Phys. Chem. A **111**, 7599 (2007).
[32] V. S. Bryantsev, M. S. Diallo, A. C. T. van Duin, and W. A. Goddard III, "Hydration of copper (II): New insights from density functional theory and the COSMO solvation model," J. Phys. Chem. A **112**, 9104 (2008).
[33] M. Bustamante, I. Valencia, and M. Castro, "Theoretical study of $[Ni(H_2O)_n]^{2+}(H_2O)_m$ (n≤6, m ≤ 18)," J. Phys. Chem. A **115**, 4115 (2011).
[34] R. Garza-Galindo, M. Castro, and M. A. Duncan, "Theoretical study of nascent hydration in the $Fe^+(H_2O)_n$ system," J. Phys. Chem. A **116**, 1906 (2012).

Published under license by AIP Publishing

[35]E. Miliordos and S. S. Xantheas, "Unimolecular and hydrolysis channels for the detachment of water from microsolvated alkaline earth dication (Mg^{2+}, Ca^{2+}, Sr^{2+}, Ba^{2+}) clusters," Theor. Chem. Acc. **133**, 1450 (2014).
[36]E. Miliordos and S. S. Xantheas, "Elucidating the mechanism behind the stabilization of multi-charged metal cations in water: A case study of the electronic states of microhydrated Mg^{2+}, Ca^{2+}, and Al^{3+}," Phys. Chem. Chem. Phys. **16**, 6886 (2014).
[37]E. Miliordos and S. S. Xantheas, "Ground and excited states of the $[Fe(H_2O)_6]^{2+}$ and $[Fe(H_2O)_6]^{3+}$ clusters: Insight into the electronic structure of the $[Fe(H_2O)_6]^{2+}$-$[Fe(H_2O)_6]^{3+}$ complex," J. Chem. Theory Comput. **11**, 1549 (2015).
[38]D. E. Lessen, R. L. Asher, and P. J. Brucat, "Vibrational structure of an electrostatically bound ion-water complex," J. Chem. Phys. **93**, 6102 (1990).
[39]M. H. Shen and J. M. Farrar, "Absorption-spectra of size-selected solvated metal-cations: Electronic states, symmetries, and orbitals in $Sr^+(NH_3)_{1,2}$ and $Sr^+(H_2O)_{1,2}$," J. Chem. Phys. **94**, 3322 (1991).
[40]K. F. Willey, C. S. Yeh, D. L. Robbins, J. S. Pilgrim, and M. A. Duncan, "Photodissociation spectroscopy of Mg^+H_2O and Mg^+D_2O," J. Chem. Phys. **97**, 8886 (1992).
[41]C. T. Scurlock, S. H. Pullins, J. E. Reddic, and M. A. Duncan, "Photodissociation spectroscopy of Ca^+-H_2O and Ca^+-D_2O," J. Chem. Phys. **104**, 4591 (1996).
[42]M. Sanekata, F. Misaizu, and K. Fuke, "Photodissociation study on $Ca^+(H_2O)_n$, n = 1–6: Electron structure and photoinduced dehydrogenation reaction," J. Chem. Phys. **104**, 9768 (1996).
[43]M. A. Duncan, "Spectroscopy of metal ion complexes: Gas phase models for solvation," Annu. Rev. Phys. Chem. **48**, 69 (1997).
[44]J. M. Farrar, "Size-dependent reactivity in open shell metal-ion polar solvent clusters: Spectroscopic probes of electronic-vibration coupling, oxidation and ionization," Int. Rev. Phys. Chem. **22**, 593 (2003).
[45]R. B. Metz, "Optical spectroscopy and photodissociation dynamics of multiply charged ions," Int. J. Mass Spectrom. **235**, 131 (2004).
[46]Y. Abate and P. D. Kleiber, "Photodissociation spectroscopy of $Zn^+(H_2O)$ and $Zn^+(D_2O)$," J. Chem. Phys. **122**, 084305 (2005).
[47]N. R. Walker, R. S. Walters, and M. A. Duncan, "Frontiers in the infrared spectroscopy of gas phase metal ion complexes," New J. Chem. **29**, 1495 (2005).
[48]H. Cox and A. J. Stace, "Recent advances in the visible and UV spectroscopy of metal dication complexes," Int. Rev. Phys. Chem. **29**, 555 (2010).
[49]J. S. Daluz, A. Kocak, and R. B. Metz, "Photodissociation studies of the electronic and vibrational spectroscopy of $Ni^+(H_2O)$," J. Phys. Chem. A **116**, 1344 (2012).
[50]A. Kocak, G. Austein-Miller, W. L. Pearson III, G. Altinay, and R. B. Metz, "Dissociation energy and electronic and vibrational spectroscopy of $Co^+(H_2O)$ and its isotopomers," J. Phys. Chem. A **117**, 1254 (2013).
[51]J. M. Lisy, "Spectroscopy and structure of solvated alkali-metal ions," Int. Rev. Phys. Chem. **16**, 267 (1997).
[52]N. R. Walker, R. S. Walters, E. D. Pillai, and M. A. Duncan, "Infrared spectroscopy of $V^+(H_2O)$ and $V^+(D_2O)$ complexes: Solvent deformation and an incipient reaction," J. Chem. Phys. **119**, 10471 (2003).
[53]R. S. Walters and M. A. Duncan, "Infrared spectroscopy of solvation and isomers in $Fe^+(H_2O)_{1,2}Ar_m$ complexes," Aust. J. Chem. **57**, 1145 (2004).
[54]Y. Inokuchi, K. Ohshimo, F. Misaizu, and N. Nishi, "Infrared photodissociation spectroscopy of $[Mg(H_2O)_{1-4}]^+$ and $[Mg(H_2O)_{1-4}Ar]^+$," J. Phys. Chem. A **108**, 5034 (2004).
[55]Y. Inokuchi, K. Ohshimo, F. Misaizu, and N. Nishi, "Structures of $[Mg(H_2O)_{1,2}]^+$ and $[Al(H_2O)_{1,2}]^+$ ions studied by infrared photodissociation spectroscopy: Evidence of $[HO\text{-}Al\text{-}H]^+$ ion core structure in $[Al(H_2O)_2]^+$," Chem. Phys. Lett. **390**, 140 (2004).
[56]N. R. Walker, R. S. Walters, M.-K. Tsai, K. D. Jordan, and M. A. Duncan, "Infrared photodissociation spectroscopy of $Mg^+(H_2O)Ar_n$ complexes: Isomers in progressive microsolvation," J. Phys. Chem. A **109**, 7057 (2005).
[57]R. S. Walters, E. D. Pillai, and M. A. Duncan, "Solvation dynamics in $Ni^+(H_2O)_n$ clusters probed with infrared spectroscopy," J. Am. Chem. Soc. **127**, 16599 (2005).
[58]T. D. Vaden, J. M. Lisy, P. D. Carnegie, E. Dinesh Pillai, and M. A. Duncan, "Infrared spectroscopy of the $Li^+(H_2O)Ar$ complex: The role of internal energy and its dependence on ion preparation," Phys. Chem. Chem. Phys. **8**, 3078 (2006).
[59]T. Iino, K. Ohashi, K. Inoue, K. Judai, N. Nishi, and H. Sekiya, "Infrared spectroscopy of $Cu^+(H_2O)_n$ and $Ag^+(H_2O)_n$: Coordination and solvation of noble-metal ions," J. Chem. Phys. **126**, 194302 (2007).
[60]P. D. Carnegie, B. Bandyopadhyay, and M. A. Duncan, "Infrared spectroscopy of $Cr^+(H_2O)$ and $Cr^{2+}(H_2O)$: The role of charge in cation hydration," J. Phys. Chem. A **112**, 6237 (2008).
[61]M. F. Bush, R. J. Saykally, and E. R. Williams, "Reactivity and infrared spectroscopy of gaseous hydrated trivalent metal ions," J. Am. Chem. Soc. **130**, 9122 (2008).
[62]M. F. Bush, R. J. Saykally, and E. R. Williams, "Infrared action spectroscopy of $Ca^{2+}(H_2O)_{11\text{-}69}$ exhibit spectral signatures for condensed-phase structures with increasing cluster size," J. Am. Chem. Soc. **130**, 15482 (2008).
[63]M. F. Bush, J. T. O'Brien, J. S. Prell, C.-C. Wu, R. J. Saykally, and E. R. Williams, "Hydration of alkaline earth metal dications: Effects of metal ion size determined using infrared action spectroscopy," J. Am. Chem. Soc. **131**, 13270 (2009).
[64]P. D. Carnegie, A. B. McCoy, and M. A. Duncan, "Infrared spectroscopy and theory of $Cu^+(H_2O)Ar_2$ and $Cu^+(D_2O)Ar_2$: Fundamentals and combination bands," J. Phys. Chem. A **113**, 4849 (2009).
[65]T. E. Cooper, J. T. O'Brien, E. R. Williams, and P. B. Armentrout, "Zn^{2+} has a primary coordination sphere of five: IR action spectroscopy and theoretical studies of hydrated Zn^{2+} complexes in the gas phase," J. Phys. Chem. A **114**, 12646 (2010).
[66]P. D. Carnegie, B. Bandyopadhyay, and M. A. Duncan, "Infrared spectroscopy of $Sc^+(H_2O)$ and $Sc^{2+}(H_2O)$ via argon complex predissociation: The charge dependence in cation hydration," J. Chem. Phys. **134**, 014302 (2011).
[67]P. D. Carnegie, B. Bandyopadhyay, and M. A. Duncan, "Infrared spectroscopy of $Mn^+(H_2O)$ and $Mn^{2+}(H_2O)$ via argon complex predissociation," J. Phys. Chem. A **115**, 7602 (2011).
[68]O. Rodriguez, Jr. and J. M. Lisy, "Revisiting $Li^+(H_2O)_{3\text{-}4}Ar_1$ clusters: Evidence of high-energy conformers from infrared spectra," J. Phys. Chem. Lett. **2**, 1444 (2011).
[69]K. Furukawa, K. Ohashi, N. Koga, T. Imamura, K. Judai, N. Nishi, and H. Sekiya, "Coordinatively unsaturated cobalt ion in $Co^+(H_2O)_n$ (n = 4–6) probed with infrared photodissociation spectroscopy," Chem. Phys. Lett. **508**, 202 (2011).
[70]J. T. O'Brien and E. R. Williams, "Coordination numbers of hydrated divalent transition metal ions investigated with IRPD spectroscopy," J. Phys. Chem. A **115**, 14612 (2011).
[71]Y. Li, G. Wang, C. Wang, and M. Zhou, "Coordination and solvation of the Au^+ cation: Infrared photodissociation spectroscopy of mass-selected $Au(H_2O)_n^+$ (n = 1–8) complexes," J. Phys. Chem. A **116**, 10793 (2012).
[72]B. Bandyopadhyay and M. A. Duncan, "Infrared spectroscopy of $V^{2+}(H_2O)$ complexes," Chem. Phys. Lett. **530**, 10 (2012).
[73]B. Bandyopadhyay, K. N. Reishus, and M. A. Duncan, "Infrared spectroscopy of solvation in small $Zn^+(H_2O)_n$ complexes," J. Phys. Chem. A **117**, 7794 (2013).
[74]H. Ke, C. van der Linde, and J. M. Lisy, "Insights into gas-phase structural conformers of hydrated rubidium and cesium cations, $M^+(H_2O)_nAr$ (M = Rb, Cs; n = 3–5), using infrared photodissociation spectroscopy," J. Phys. Chem. A **118**, 1363 (2014).
[75]T. B. Ward, P. D. Carnegie, and M. A. Duncan, "Infrared spectroscopy of the $Ti(H_2O)Ar^+$ ion-molecule complex: Electronic state switching induced by argon," Chem. Phys. Lett. **654**, 1 (2016).
[76]T. B. Ward, E. Miliordos, P. D. Carnegie, S. S. Xantheas, and M. A. Duncan, "Ortho-para interconversion in cation-water complexes: The case of $V^+(H_2O)$ and $Nb^+(H_2O)$ clusters," J. Chem. Phys. **146**, 224305 (2017).
[77]M. A. Duncan, "Metal cation coordination and solvation studied with infrared spectroscopy in the gas phase," in *Physical Chemistry of Cold Gas Phase Functional Molecules and Clusters*, edited by T. Ebata and M. Fujii (Springer, Berlin, 2019), p. 157.
[78]P. D. Carnegie, J. H. Marks, A. D. Brathwaite, T. B. Ward, and M. A. Duncan, "Microsolvation in $V^+(H_2O)_n$ clusters studied with selected-ion infrared spectroscopy," J. Phys. Chem. A **124**, 1093 (2020).
[79]D. Lessen and P. J. Brucat, "Resonant photodissociation of $CoAr^+$ and $CoKr^+$: Analysis of vibrational structure," J. Chem. Phys. **90**, 6296 (1989).
[80]C. W. Bauschlicher, Jr., H. Partridge, and S. R. Langhoff, "Theoretical study of metal noble-gas positive ions," J. Chem. Phys. **91**, 4733 (1989).

Published under license by AIP Publishing

[81] D. Bellert and W. H. Breckenridge, "Bonding in ground-state and excited-state A^+Rg van der Waals ions (A = atom, Rg = rare gas atom): A model-potential analysis," Chem. Rev. **102**, 1595 (2002).
[82] J. D. Mosley, T. C. Cheng, S. D. Hasbrouck, A. M. Ricks, and M. A. Duncan, "Electronic spectroscopy of $CoNe^+$ via mass-selected photodissociation," J. Chem. Phys. **135**, 104309 (2011).
[83] M. A. Duncan, "Laser vaporization cluster sources," Rev. Sci. Instrum. **83**, 041101 (2012).
[84] M. A. Duncan, "Reflectron time-of-flight mass spectrometer for laser photodissociation," Rev. Sci. Instrum. **63**, 2177 (1992).
[85] H.-J. Werner, P. J. Knowles, G. Knizia, F. R. Manby, M. Schütz, P. Celani, W. Györffy, D. Kats, T. Korona, R. Lindh, A. Mitrushenkov, G. Rauhut, K. R. Shamasundar, T. B. Adler, R. D. Amos, S. J. Bennie, A. Bernhardsson, A. Berning, D. L. Cooper, M. J. O. Deegan, A. J. Dobbyn, F. Eckert, E. Goll, C. Hampel, A. Hesselmann, G. Hetzer, T. Hrenar, G. Jansen, C. Köppl, S. J. R. Lee, Y. Liu, A. W. Lloyd, Q. Ma, R. A. Mata, A. J. May, S. J. McNicholas, W. Meyer, T. F. Miller III, M. E. Mura, A. Nicklaß, D. P. O'Neill, P. Palmieri, D. Peng, K. Pflüger, R. Pitzer, M. Reiher, T. Shiozaki, H. Stoll, A. J. Stone, R. Tarroni, T. Thorsteinsson, M. Wang, and M. Welborn, MOLPRO, Version 2019.2 (2010).
[86] M. J. Frisch, G. W. Trucks, H. B. Schlegel, G. E. Scuseria, M. A. Robb, J. R. Cheeseman, G. Scalmani, V. Barone, G. A. Petersson, H. Nakatsuji, X. Li, M. Caricato, A. V. Marenich, J. Bloino, B. G. Janesko, R. Gomperts, B. Mennucci, H. P. Hratchian, J. V. Ortiz, A. F. Izmaylov, J. L. Sonnenberg, D. Williams-Young, F. Ding, F. Lipparini, F. Egidi, J. Goings, B. Peng, A. Petrone, T. Henderson, D. Ranasinghe, V. G. Zakrzewski, J. Gao, N. Rega, G. Zheng, W. Liang, M. Hada, M. Ehara, K. Toyota, R. Fukuda, J. Hasegawa, M. Ishida, T. Nakajima, Y. Honda, O. Kitao, H. Nakai, T. Vreven, K. Throssell, J. A. Montgomery, Jr., J. E. Peralta, F. Ogliaro, M. J. Bearpark, J. J. Heyd, E. N. Brothers, K. N. Kudin, V. N. Staroverov, T. A. Keith, R. Kobayashi, J. Normand, K. Raghavachari, A. P. Rendell, J. C. Burant, S. S. Iyengar, J. Tomasi, M. Cossi, J. M. Millam, M. Klene, C. Adamo, R. Cammi, J. W. Ochterski, R. L. Martin, K. Morokuma, O. Farkas, J. B. Foresman, and D. J. Fox, Gaussian 16, Revision C.01 (Gaussian, Inc., Wallingford CT, 2016).
[87] H. S. Yu, X. He, S. L. Li, and D. G. Truhlar, "MN15: A Kohn-Sham global-hybrid exchange-correlation density functional with broad accuracy for multi-reference and single-reference systems and noncovalent interactions," Chem. Sci. **7**, 5032 (2016).
[88] T. Shimanouchi, "Molecular vibrational frequencies," in *NIST Chemistry WebBook*, NIST Standard Reference Database Number 69, edited by P. J. Linstrom and W. G. Mallard (National Institute of Standards and Technology, Gaithersburg MD, 20899, retrieved, 2020).
[89] C. M. Western, "A program for simulating rotational, vibrational and electronic spectra," J. Quant. Spectrosc. Radiat. Transfer **186**, 221 (2017).
[90] M. A. Duncan, "Infrared laser spectroscopy of mass-selected carbocations," J. Phys. Chem. A **116**, 11477 (2012).
[91] P. J. Kelleher, C. J. Johnson, J. A. Fournier, M. A. Johnson, and A. B. McCoy, "Persistence of free internal rotation in $NH_4^+(H_2O)\cdot He_{n=0-3}$ ion-molecule complexes: Expanding the case for quantum delocalization in He tagging," J. Phys. Chem. A **119**, 4170–4176 (2015).

Published under license by AIP Publishing